

## Research Article

# Simple Evaluation of the Nonlinearity Signature of an ADC Using a Spectral Approach

E. J. Peralías, M. A. Jalón, and A. Rueda

*Centro Nacional de Microelectrónica (CNM-CSIC), Instituto de Microelectrónica de Sevilla (IMSE), University of Sevilla, Edificio CICA, Avenue Reina Mercedes s/n, 41012 Sevilla, Spain*

Correspondence should be addressed to E. J. Peralías, peralias@imse.cnm.es

Received 17 October 2007; Revised 30 March 2008; Accepted 16 May 2008

Recommended by Marcelo Lubaszewski

This work presents a new method to estimate the nonlinearity characteristics of analog-to-digital converters (ADCs). The method is based on a nonnecessarily polynomial continuous and differentiable mathematical model of the converter transfer function, and on the spectral processing of the converter output under a sinusoidal input excitation. The simulation and experiments performed on different ADC examples prove the feasibility of the proposed method, even when the ADC nonlinearity pattern has very strong discontinuities. When compared with the traditional code histogram method, it also shows its low cost and efficiency since a significant lower number of output samples can be used still giving very realistic INL signature values.

Copyright © 2008 E. J. Peralías et al. This is an open access article distributed under the Creative Commons Attribution License, which permits unrestricted use, distribution, and reproduction in any medium, provided the original work is properly cited.

## 1. INTRODUCTION

The parameters that characterize the transfer function of an ADC, such as the integral nonlinearity (INL), are some of the most important specifications that must be known to insure the correct operation of the ADC in a certain application. One of the standardized methods to estimate these parameters is the code histogram test [1, 2]. Its main drawback is the excessive cost of its application, especially due to the large number of samples that must be acquired (more than one million) and to the fact that this number increases, in general, in an exponential way with the number of bits of the ADC. The synchronization between the acquisition and the signal stimulation is also a nonelemental task. On the contrary, this method can achieve a very precise measurement independently of the shape of the transfer characteristic; it is a clear trade-off between time and precision.

These drawbacks make the histogram method unfeasible for low-speed and high-resolution converters (>15 bits). For these kinds of converters, the use of methods based on spectral processing can be satisfactory acquiring only some tens of thousands of samples independently of the ADC resolution [3–6]. Although this estimate leads to a partial description of the static behavior of the ADC and,

for example, it is not a reliable method to calibrate the nonlinearity, such description may be enough to show a malfunctioning and it may be very useful to set a test protocol [7–9].

This paper presents a new and simple method for ADC nonlinearity (INL) estimation using the spectral processing of its response to a sine-wave excitation. The method does not require a concrete functional form for the ADC transfer curve or for the INL, as [3, 4], nor to apply specific expansion series as in [6], although it is based on a continuous and differentiable mathematical model of the converter transfer function. To reach high precision in the INL estimation, the transfer function should have enough smooth shape; however, we will show that it can be also applied in many cases with strong discontinuities, giving INL signatures good enough to describe the nonlinear behavior of the ADC, this validating its use for rapid production test. The mathematical bases of this method are the standard definition of the INL and the local variation of the ADC transfer function around each ideal transition.

The organization of this paper is as follows. Section 2 introduces the general hypotheses to apply the new method and the mathematics to obtain the INL signature. The method adaptation for its application through the spectral estimation is derived in Section 3. Section 4 shows some

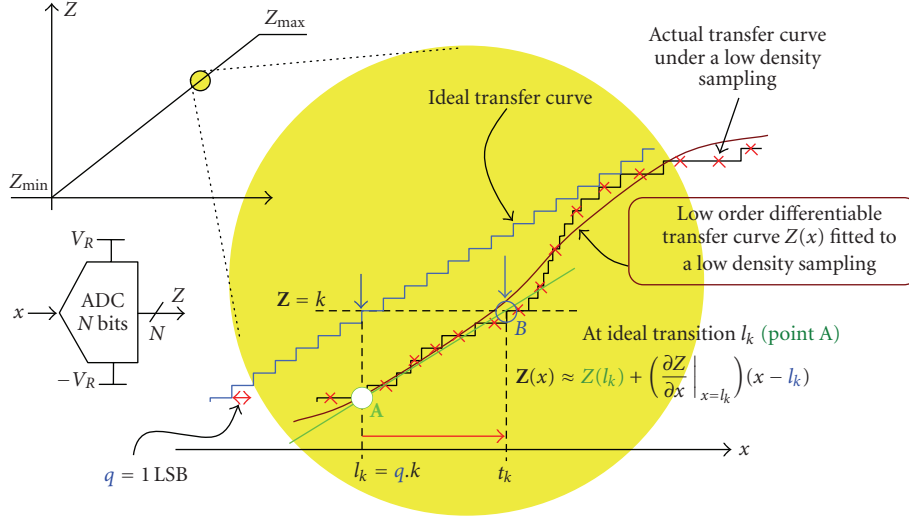


FIGURE 1: Modelling the non-linearity: the first order Taylor's expansion of the transfer function  $Z(x)$  around an ideal transition  $l_k$ .  $t_k$  represents the real transition where the output code  $Z$  changes from  $k - 1$  to  $k$ .

simulated and real examples of application for the proposed method and Section 5 draws the conclusions.

## 2. MODELLING THE NONLINEARITY

The ADC basic model that we are considering supposes that the transfer curve: (1) is a smooth nonnecessarily polynomial function  $Z(x)$ , continuous and differentiable with respect to the input, (2) it must be strictly increasing and therefore with a nonzero derivative. The description as a continuous function must be also understood in the way that the resolution of the converter is high enough to consider the quantization effect embedded in other noise contributions.

Mathematically, the proposed input-output model is

$$z = Z(x) + \varepsilon(x), \quad \exists \partial_x Z \neq 0, \quad \forall x \in [-V_R, V_R], \quad (1)$$

where the error function  $\varepsilon(x)$  is of the same order than the quantization error. Without any loss of generality, the input range will be considered bipolar and centred at zero,  $[-V_R, V_R]$ .

Figure 1 illustrates the nonlinearity modeling. Both the ideal and a hypothetic real transfer function of an  $N$ -bit converter are shown. The curve  $Z(x)$  is that obtained by fitting a low-density sampling of the real transfer curve. Considering the previous conditions, a first-order Taylor's expansion of the mild transfer function  $Z(x)$  is going to be calculated around each ideal transition,  $l_k$ . The set of points formed by the ideal transitions can be expressed as  $l_k = q \cdot k$ ,  $k \in [-2^{N-1}, 2^{N-1} - 1]$ , where  $q = 2V_R/2^N$  is the LSB of the  $N$ -bit ADC. Then, we have

$$Z(x) \approx Z(l_k) + \partial_x Z(l_k) \cdot (x - l_k), \quad \forall x \approx l_k. \quad (2)$$

Evaluating the expression at the corresponding real transition,  $x = t_k$ , where the output code value changes from  $k - 1$  to  $k$ ,

$$k \approx Z(l_k) + \partial_x Z(l_k) \cdot q \text{INL}_k, \quad (3)$$

where it has been used that  $k \approx Z(t_k)$  and the standard INL definition  $\text{INL}_k = (t_k - l_k)/q$  [1].

From (3), the following expression for the INL can be obtained:

$$\text{INL}_k \approx \frac{k - Z(l_k)}{q \partial_x Z(l_k)}. \quad (4)$$

Notice that this expression can be evaluated only if it is possible to obtain the derivative of the function  $Z(x)$ .

If the second derivative exists, an alternative expression can be obtained using the second-order Taylor's expansion. In any case, in this work only the expression (4) will be used since the nonlinearity of the ADC is considered very small:  $\max_k \{|\text{INL}_k|\} < 2^{N-10}$  ( $N > 10$ ).

## 3. APPLICATION OF THE MODEL USING A SPECTRAL APPROACH

This section shows how to apply expression (4) in the case that a spectral measurement is used to process the ADC response to a sinusoidal input.

Let us assume that the input excitation is

$$x(t) = A \cos(\omega_x t + \varphi_x) + B \quad (5)$$

and that it covers all the input range without causing the ADC saturation ( $A \approx V_R$ ,  $B \approx 0$ ). The input frequency  $\omega_x$  is low enough to produce unimportant dynamic effects. The phase-shift  $\varphi_x$  and the offset  $B$  do not need to be known a priori. The amplitude,  $A$ , has to be known only when the gain of the ADC,  $g$ , is very different from the unity and/or it is wanted to estimate the gain error of the A/D conversion.

For such input, the ADC output is a superposition of harmonics of the excitation frequency,

$$Z(x(t)) = C_0 + \sum_{n \geq 1} C_n \cos(\omega_n t + \varphi_n), \quad \omega_n = n\omega_1, \quad (6)$$

where the frequency  $\omega_x$  and the phase-shift  $\varphi_x$  are identified with the frequency  $\omega_1$  and the phase-shift  $\varphi_1$  of the main harmonic, respectively. Rejecting, in a first approximation, the other harmonics ( $n > 1$ ), the input amplitude can also be related to the amplitude of the 1st harmonic by means of the gain  $g$  of the ADC. Using a simple linear model  $Z(x) \approx (g \cdot x)/q + z_{os}$ , where  $g$  is the gain and  $z_{os}$  is the offset of the ADC [1], it can be obtained as follows:

$$\begin{aligned} C_1 &= g \cdot A/q, \\ C_0 &= (g \cdot B)/q + z_{os}, \\ \omega_1 &= \omega_x, \\ \varphi_1 &= \varphi_x. \end{aligned} \quad (7)$$

A more suitable model, but more costly, could still use the previous linear relationship but considering as outputs the sine-wave signal  $\hat{z}(t) = C_A \cos(\omega_z t + \varphi_z) + C_B$  that best fits to (6) in the sense of the least mean-squared error. In this case, expressions (7) are still valid using the parameters  $C_A$ ,  $C_B$ ,  $\omega_z$ , and  $\varphi_z$ . In any case, whatever the model is, the transfer function derivative in (4) can now be calculated in an indirect way:

$$\begin{aligned} \partial_x Z &= \frac{\partial_t Z(x(t))}{\partial_t x(t)} = \frac{\sum_{n \geq 1} \omega_n C_n \sin(\omega_n t + \varphi_n)}{\omega_x A \sin(\omega_x t + \varphi_x)} \\ &\approx \frac{g}{q} \left[ 1 + \sum_{n \geq 2} \frac{C_n}{C_1} \frac{n \sin(n\omega_1 t + \varphi_n)}{\sin(\omega_1 t + \varphi_1)} \right], \end{aligned} \quad (8)$$

where the relations in (7) have been applied to the simplest model.

Now, let us evaluate expressions (6) and (8) at the ideal transitions,  $Z(l_k)$ ,  $\partial_x Z(l_k)$ .

If  $\tau_k$  are the time instants in which the sinusoidal input signal crosses the ideal transitions of the ADC,  $x(\tau_k) = l_k$  (see Figure 2), it can be written as

$$\begin{aligned} l_k &= A \cos(\omega_x \tau_k + \varphi_x) + B \\ \rightarrow \omega_x \tau_k &= -\varphi_x + \text{Arccos}\left(\frac{l_k - B}{A}\right). \end{aligned} \quad (9)$$

Applying relations (7),

$$\delta_k = \omega_1 \tau_k \approx -\varphi_1 + \text{Arccos}\left(\frac{g \cdot k + z_{os} - C_0}{C_1}\right) \quad (10)$$

that gives the phases used in (6) and (8)

$$\omega_n t + \varphi_n|_{t=\tau_k} = n\omega_1 \tau_k + \varphi_n = n\delta_k + \varphi_n \quad (11)$$

to obtain, respectively,  $Z(l_k)$  and  $\partial_x Z(l_k)$ . Finally, expression (4) for the INL becomes

$$\text{INL}_k \approx \frac{k - \left(C_0 + \sum_{n \geq 1} C_n \cos(n\delta_k + \varphi_n)\right)}{g \cdot \left[1 + \sum_{n \geq 2} (C_n/C_1) (n \sin(n\delta_k + \varphi_n) / \sin(\delta_k + \varphi_1))\right]}. \quad (12)$$

Notice that in (10) and (12) the only quantities to evaluate are the harmonic amplitudes  $\{C_n\}$ , the phase-shifts  $\{\varphi_n\}$ ,

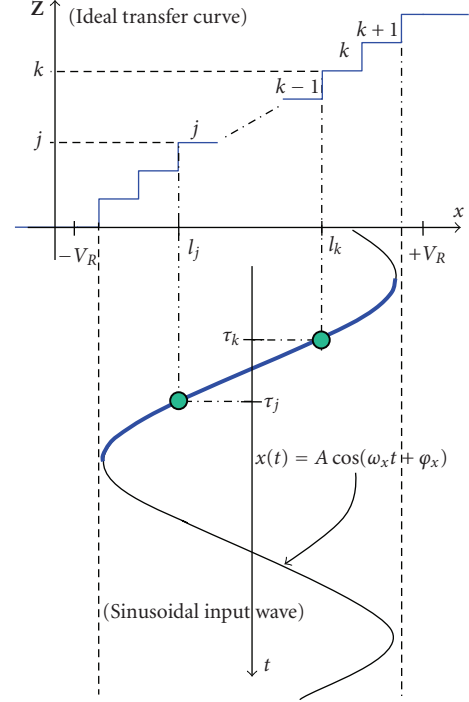


FIGURE 2: Defining the input wave crossing points  $\tau_k$  over the ADC ideal transitions  $l_k$ . According to (10), these timing points allow work out the phase values of the output harmonics when the input wave crosses an ideal transition.

and the gain  $g$  of the ADC. All of them can be estimated using the spectral processing of the output. In general,  $z_{os}$  in (10) can be considered null, which is equivalent to consider that  $z_{os}$  is cancelled out by the input offset. When  $g = 1$  and  $z_{os} = 0$  are used in (10) and (12), the ADC intrinsic nonlinearity is being estimated, that is, the nonlinearity signature without gain and offset effects. This is the INL usually evaluated according to the standards [1, 2].

The number of harmonics that must be selected to apply (12) depends on both the spectral discrimination that the total noise allows and the reliability of the mathematical method used to estimate the harmonic parameters. In all of our experiments, we have used a conservative criterion: the selected harmonics are those with amplitudes at least 10 dB over the spectrum noise floor. Mathematical methods to estimate spectra are basically based on discrete-time Fourier transform (DTFT) [1, 2].

In very good coherent experiments (input frequency and sampling frequency are commensurable values), and when the noise is small enough and well described by additive white model, simple relationships can be used. Being acquired  $L$  samples of the ADC output,  $\{z_i\}_{i=1}^L$ , with the sampling frequency  $f_s$  and satisfying the input wave frequency  $f_x = (M/L)f_s$  with  $M$  and  $L$  relative prime integers (to excite at least  $L$  ADC different levels), the DTFT is obtained of the output register,  $\{\zeta_j\} = \text{FFT}\{z_i\}$ , selecting after that the most significant spectral lines respect to the noise floor,  $\{\zeta_n\}_{n=1}^H$ . The main harmonic occurs at  $j_1 = M$ . The correct frequencies for the other lines must be

carefully identified because if high-order harmonics exist,  $\omega_n > \omega_s/2$ , their spectral lines are folded at the DTFT interval  $[0, f_s/2]$ . With these considerations, expressions to estimate the parameters involved in (12) are

$$\begin{aligned}\omega_1 &= 2\pi f_s M/L, \\ \omega_n &= n\omega_1, \\ C_0 &= \text{mean}_i(\{z_i\}), \\ C_n &= (2/L)\|\zeta_{j_n}\|, \\ \varphi_n &= (-1)^{p_n} \text{Arg}(\zeta_{j_n}), \\ p_n &= \begin{cases} 0, & \omega_n/\omega_s \in [k, (2k+1)/2], \\ 1, & \omega_n/\omega_s \in [(2k+1)/2, (k+1)], \end{cases} \\ g &= q \cdot \text{rms}\{z_i\} / \text{rms}\{x(t)\},\end{aligned}\quad (13)$$

where  $\text{rms}\{x(t)\}$  is the root mean square of the input wave and  $p_n$  corrects the inversion of estimated phase for the case that a spectral line is folded.

Although it has been suggested about (12) that the value of the gain  $g$  is not strictly necessary for the intrinsic nonlinearity evaluation, in (13) it has been included an expression that uses the root mean square for its estimation. This expression allows a simple way to evaluate  $g$  because it is easy to measure the rms value of the input signal using a wattmeter. For a low-distortion ADC (such as it has been considered for the application of the method), the difference of the gain value estimated using this way is usually less than 0.5% respect to the gain value estimated using a standardized method, such as that estimating  $g$  through the slope of the best-fitting line to the transition set, or the slope of the straight line that joins the extreme transitions on the ADC transfer function [1].

If  $R$  registers ( $R > 1$ ) of length  $L$  are acquired to average the noise, all of them must be consecutively taken to do not lose the phase information. This is the same as to trace a unique register with  $R \cdot L$  output samples of  $L$ -sample periodicity. In this way, (13) is still used but with the averaged module and the averaged phase spectrum values,

$$\begin{aligned}\overline{\|\zeta_j\|} &= \sqrt{\text{mean}_{m=1,\dots,R}\{\|\zeta_j^{(m)}\|^2\}}, \\ \overline{\text{Arg}(\zeta_j)} &= \text{mean}_{m=1,\dots,R}\{\text{Arg}(\zeta_j^{(m)})\}, \\ \text{with } \{\zeta_j^{(m)}\}_{m=1}^R &= \text{FFT}\{z_i^{(m)}\}.\end{aligned}\quad (14)$$

If a coherent sampling is not possible, *windowing* to each register should be applied to reduce the spectral leakage,  $\{\zeta_j^{(m)}\}_{m=1}^R = \text{FFT}\{w_i z_i^{(m)}\}$ , where  $\{w_i\}_{i=1}^L$  is the convolution window. In general, the expressions in (13) have to be corrected since the estimates are biased depending on the applied window. In [2, 10], there are some suggestions to select the most appropriate window. For all of our noncoherent experiments, we have used a 4-term cosine-class window and an estimation method based on phase regression presented in [11], which requires that  $R \geq 2$ .

When high-order harmonics exist and they are folded in the  $[0, f_s/2]$  band, a particular input frequency has to be selected in such a way that no significant harmonic overlaps. Problems are minor if coherent sampling and no windowing are applied. We have always selected test frequencies that lead spectral lines to separate each other at least 10 bins, when 4-term cosine window has been used.

The DC component is evaluated by means of the weighted mean of the samples, using as weight function the convolution window,

$$C_0 = \text{mean}_m \left\{ \frac{\sum_i w_i z_i^{(m)}}{\sum_i w_i} \right\}. \quad (15)$$

## 4. APPLICATION EXAMPLES

### 4.1. Simulated experiments

This section shows the simulation results obtained applying the introduced method in two different models for the ADC. The first converter, ADC<sub>1</sub>, has a very regular transfer curve and a smooth INL. For the second one, ADC<sub>2</sub>, the transfer curve is nonmonotonic and its INL has very strong discontinuities.

#### 4.1.1. Nonspectral approach (DC sweep) on low-speed, high-resolution ADC<sub>1</sub> model

Before applying (12), let us show the immediate approximation of (4). The ADC<sub>1</sub> has been excited using a DC signal whose value is changing inside the input range. For each value of the input,  $\bar{x}_i$ , it is obtained an output register to calculate the corresponding average code  $\bar{z}_i$ . Using the set  $\{(\bar{x}_i, \bar{z}_i)\}$  it can be built the  $M$ th order best-fitting polynomial model,  $Z_M(x)$ , which allows to apply (4) directly.

ADC<sub>1</sub> is a high-level model of a 14-bit  $\Sigma\Delta$  converter, with reference voltages 0.0 V and 5.0 V but with a practical input range [0.5 V, 4.5 V]. The model reproduces the nonlinear, noisy, and frequency behavior. The sampling frequency is  $f_s = 100$  kHz. The noise due to both the input and the ADC, referred to the input, is approximately 2LSBs rms white noise. A DC sweep with about 4000 points has been carried out in the range [0.7 V, 4.3 V]. For each DC value, it has been taken a register of 50 points, being the obtained code in the range  $Ik = [-5792, 5801]$ . Using this dataset, the  $M = 32$ nd-order best-fitting polynomial has been calculated by means of the first class Chebyshev base. The choice of the order is deduced from the harmonic significant number found in the experiment that will be described in next subsection. For each value  $k$  of  $Ik$ , it has been evaluated  $Z_M(l_k)$ ,  $\partial_x Z_M(l_k)$ , and  $\text{INL}_k$  in (4).

On the other hand, it has been applied the standard sinusoidal histogram method [1, 2] to determine a good estimate of the INL (*real INL* from now on) in order to establish a reference for comparison purpose. The obtained results are depicted in Figure 3.

Figure 3(a) shows the superposition of both estimates. The thick line is the curve calculated by (4). To show the reliability achieved, in Figure 3(b) it is depicted the difference

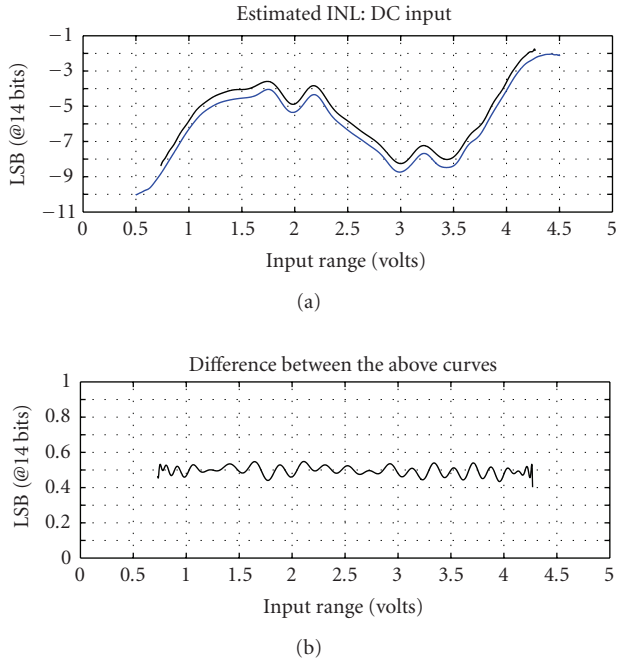


FIGURE 3: (a) INL estimates of the example  $ADC_1$ . In thick (black) line the one obtained by (4), in thin (blue) line the *real INL* evaluated by the Histogram method. (b) Differences between both estimates in (a).

between both curves, which is affected by a systematic 1/2 LSB error. This is because, for convenience, (2) and (3) have been obtained using the transitions and not the code centres. This is not very important since, in general, the offset value of the ADC is not used in the expression (12) and so it must be corrected by means of the elimination of its mean value. In any way, it can be noticed the high accuracy achieved by the method. This is justifiable since the INL curve of this ADC follows a very smooth behavior.

#### 4.1.2. Spectral approach (sine input) on low-speed, high-resolution $ADC_1$ model

For the same  $ADC_1$  converter, it has been simulated a set of 35 experiments that use a sinusoidal input and calculate the INL from (12). To estimate the parameters from the spectrum, it has been used the procedure described in [11]. The amplitude of the sinusoidal input is approximately  $-3$  dBFS, the offset is about 100LSBs, and the frequency is near  $f_s/83$ . The phase has been evenly spread inside the range  $[-\pi, \pi]$  all over the experiments. The equivalent noise at the input is approximately 1LSB rms white noise. In each experiment,  $R = 4$  consecutive registers of  $L = 4096$  samples are used. A set of 500 samples have been eliminated at the beginning of the four registers to reduce the settling errors. A typical spectrum is shown in Figure 4(a). As the background noise is about  $-112$  dBFS, the spectral lines selected are those that have the amplitude higher than  $-102$  dBFS. The typical selection detects about 15 harmonics with orders up to 30th. Figure 4(b) shows a comparison between the *real INL*

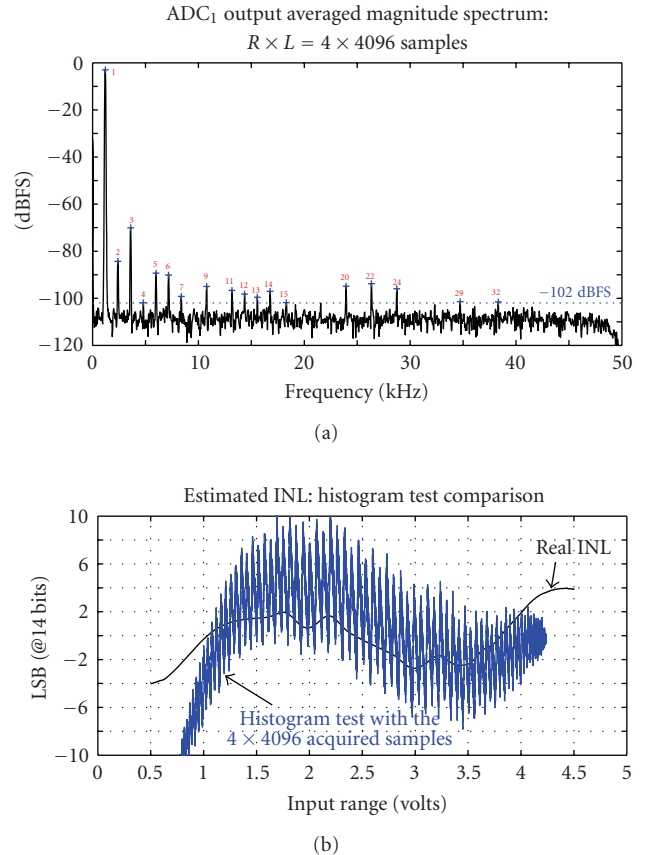


FIGURE 4: (a) Typical averaged magnitude spectrum obtained from the  $ADC_1$  output. It is used for the selection of the spectral lines taken as harmonics. (b) Comparison between two  $ADC_1$  INL Histogram estimations: in thin (blue) line the one estimated with very few samples, (the four registers acquired to apply the new method). In thick (black) line the *real INL*.

(thick line) and the estimated (thin line) using the histogram method but with only the above four acquired registers. It is obvious that the number of acquired samples is not still enough to sketch the INL shape. On the other hand, the results obtained in one of the experiments using the spectral estimation and (12) are shown in Figures 5(a) and 5(b). As it can be noticed, our method gives good enough results with the 4·4096 acquired samples. Both INL curves have been depicted with the offset corrected, since the offset of the  $ADC_1$  has been supposed null  $z_{os} = 0$ . To show how robust the estimate from (12) is, Figure 5(c) depicts the differences between the INL of each experiment and the *real INL*.

#### 4.1.3. Spectral approach (sine input) on medium-speed, high-resolution model $ADC_2$

The  $ADC_2$  is a high-level model of a 16-bit pipeline converter that operates with reference voltages of  $-2.0$  V and  $2.0$  V. The sampling frequency is  $f_s = 5.0$  MHz. The noise due to both the input and the ADC, referred to the input, is approximately 1LSB rms white noise. The amplitude of the



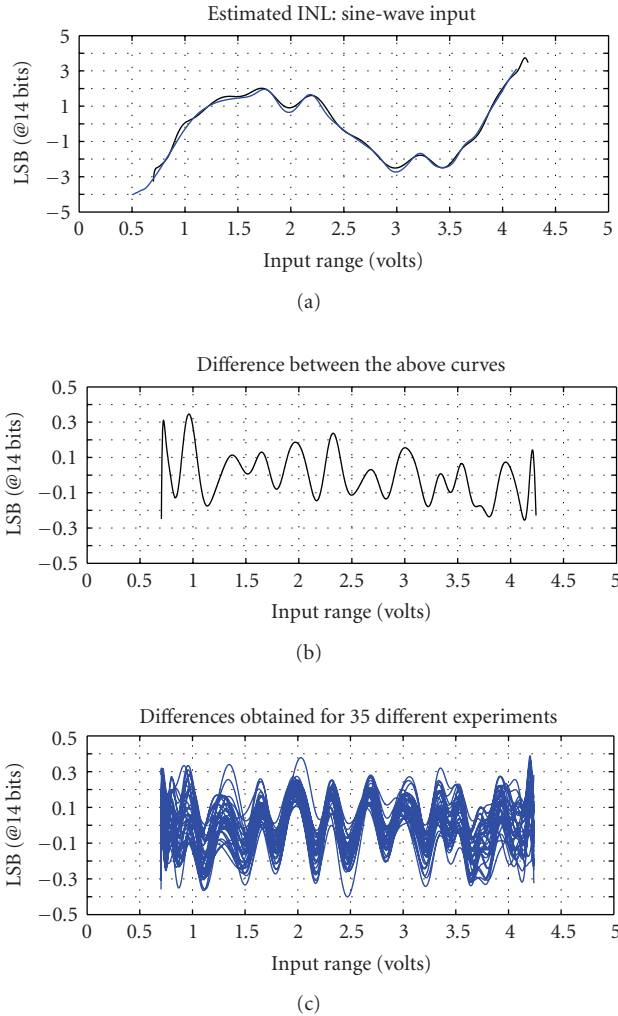


FIGURE 5: (a) Overlapped  $ADC_1$  INL curves: in thick (black) line the one obtained by spectral estimation and (12). In thin (blue) line the *real INL*. (b) Difference between the two above INL signatures. (c) Differences obtained for all of the experiments on the  $ADC_1$ .

input signal is approximately  $-0.2$  dBFS, the offset is about 10LSBs and the frequency is near  $f_s/222$ .

The phase has been evenly spread all over the experiments inside the range  $[-\pi, \pi]$ . In these experiments, it has been taken two consecutive registers with 32768 samples each. In this example, the background noise appears at about  $-130$  dBFS, so the selected spectral lines are those that are harmonics with amplitudes higher than  $-120$  dBFS.

The so irregular and discontinuous structure of the INL of this ADC leads to a typical selection about 150 harmonics with orders up to 600th. Figure 6 shows the typical results obtained. Figure 6(a) shows a comparison between the *real INL* (thick line) and the one estimated (thin line) using the histogram method with the above two acquired registers. The number of acquired samples is not still enough to sketch the INL shape. However and in spite of such a discontinuous structure of the nonlinearity of the  $ADC_2$ , the estimate from (12) absolutely follows the *real*

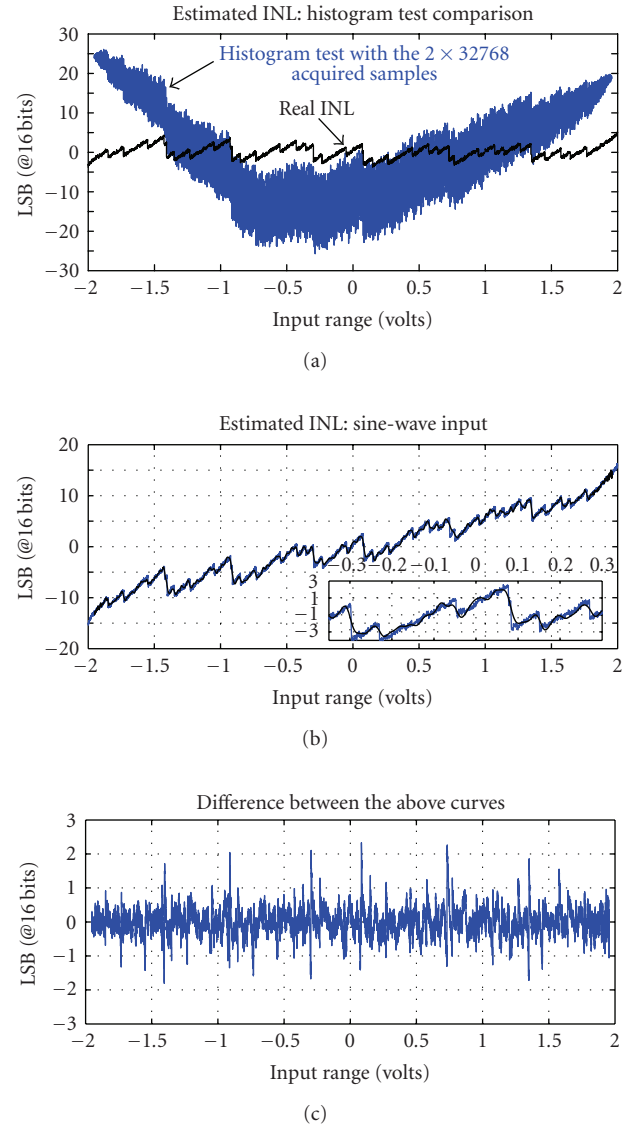


FIGURE 6: (a) Comparison between two  $ADC_2$  INL Histogram estimations: in thin (blue) line the one estimated with very few samples (the two registers acquired to apply the new method). In thick (black) line the *real INL*, (no gain effect has been included). (b) Overlapped  $ADC_2$  INL estimations: the estimated using the spectral approach and (12), and the *real INL* (gain effects are included). (c) Difference between the above INL signatures in (b).

INL evaluated using the standardized histogram method (Figure 6(b)). The difference between both estimates has been depicted in Figure 6(c). Biggest differences occur at the higher transitions, where the smoothing effect due to the limited number of harmonics that has been selected is more evident. Even if the gain is not evaluated, the intrinsic nonlinearity of the ADC (the one where the gain and the offset are corrected) still can be extracted. Figure 7(a) shows the results obtained for the  $ADC_2$  making  $g = 1$  in (10). Although the difference is noticeable, if the gain and offset are eliminated from both curves (subtracting their best-

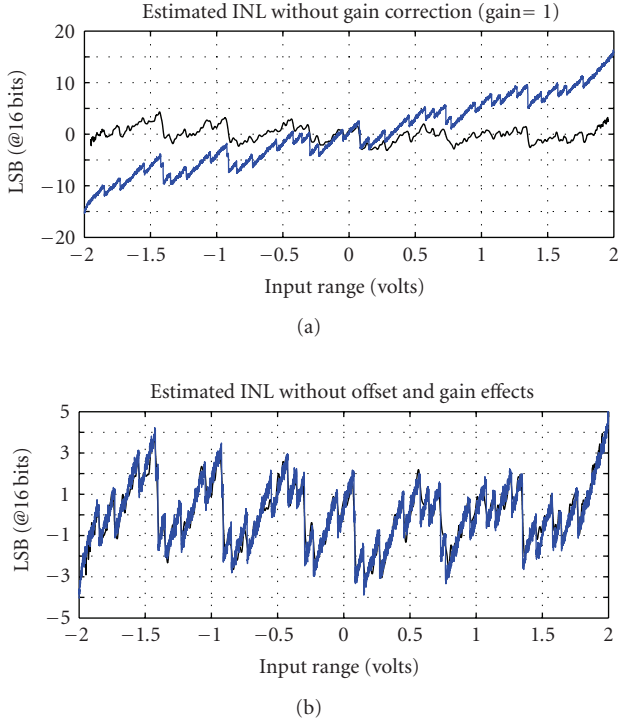


FIGURE 7: (a) Thick (black) line: estimated  $ADC_2$  INL using (12) and taking the gain equal to 1. In thin (blue) line the *real INL* where gain effects are included. (b) Overlapping of the two above estimations after the gain and offset effects have been corrected.

fitting lines), a good approximation can be achieved as Figure 7(b) shows.

## 4.2. Real experiments

This section shows the results obtained applying the introduced method to a real ADC. This converter has a transfer curve with very strong discontinuities.

### 4.2.1. Spectral approach (sine input) on high-speed, low-voltage experimental prototype ADC

The ADC under test is a fully differential 12-bit pipeline converter prototype in a 120 nm CMOS technology with reference voltages  $-1$  V and  $1$  V. The sinusoidal input has been nonbuffered AC coupled to the ADC and generated using the Agilent N8241A AWG, with amplitude of  $-0.1$  dBFS and a frequency of  $500$  kHz approximately. In this case, as a good coherent experiment has been done, only a register of  $4090$  samples has been acquired using a  $20$  MHz sampling master clock (neither averaging nor windowing has been applied). Figure 8(a) shows a typical nonwindowed magnitude spectrum, with the floor noise at about  $-100$  dBFS. The harmonics selected were those with the amplitude higher than  $-90$  dBFS, and the typical selection takes about  $45$  harmonics with orders up to  $150$ th.

Figure 8(b) compares the INL pattern obtained using the spectral approach (from (12)) with the *real INL* estimated

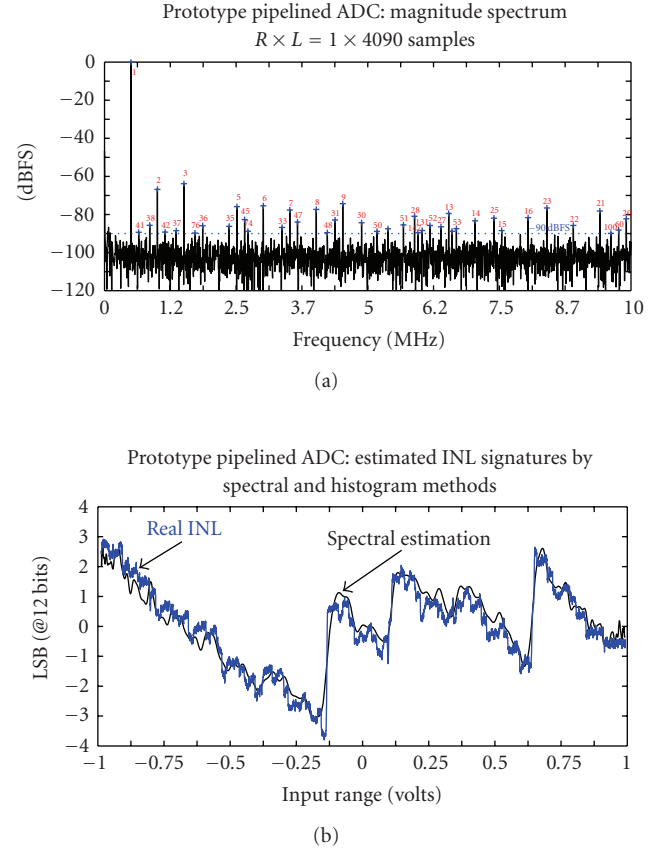


FIGURE 8: (a) Typical magnitude spectrum obtained from the prototype Pipeline ADC output. (b) Comparison between two INL estimations: In thin (blue) line, the *real INL*. In thick (black) line the INL estimation from the spectral approach and (12) using the spectrum in (a) (gain and offset effects have been corrected).

using the standard histogram method. Notice that the INL evaluated from our proposed method describes the shape of the *real INL* good enough, even in hard discontinuities. Best results are obtained if more registers have been acquired, since noise averaging improves both uncertainty and the number of selected harmonics.

## 5. CONCLUSIONS

In this paper, a new method for the INL estimation of ADCs has been presented which is based on a continuous model of the ADC transfer function. The method uses a spectral processing of the ADC output to estimate its harmonic amplitudes and phase-shifts from which the INL signature is derived. Different ADC examples with very different nonlinearity pattern have been performed to validate the proposed method. The obtained results have been compared with those obtained from the traditional histogram method and have proven not only the feasibility of the new method, even when the ADC nonlinearity has very strong discontinuities, but also its low cost and efficiency since a significant lower number of output samples can be used still giving very realistic INL signature values.

## ACKNOWLEDGMENTS

The authors would like to thank Jesús Ruiz and Dr. Manuel Delgado, both from Microelectronic Institute of Seville, to allow the application of our method to their prototype ADC exposed in Section 4.2. This work is in part supported by the Spanish Project TEC2007-68072 and the Andalusian Project EXC/2005/TIC-927.

## REFERENCES

- [1] IEEE standard 1241-2000 for terminology and test methods for analog-to-digital converters, December 2000.
- [2] European Project DYNAD—SMT4-CT98-2214, “Methods and draft standards for the dynamic characterization and testing of ADCs,” Version 3.3, September 2000, <http://paginas.fe.up.pt/~hsm/dynad/>.
- [3] F. Adamo, F. Attivissimo, N. Giaquinto, and M. Savino, “Measuring the static characteristic of dithered A/D converters,” *Measurement*, vol. 32, no. 4, pp. 231–239, 2002.
- [4] F. Attivissimo, N. Giaquinto, and I. Kale, “INL reconstruction of A/D converters via parametric spectral estimation,” *IEEE Transactions on Instrumentation and Measurement*, vol. 53, no. 4, pp. 940–946, 2004.
- [5] V. Kerzérho, S. Bernard, J. M. Janik, and P. Cauvet, “Comparison between spectral-based methods for INL estimation and feasibility of their implantation,” in *Proceedings of the 11th IEEE International Mixed-Signal Testing Workshop (IMSTW '05)*, pp. 270–275, Cannes, France, June 2005.
- [6] J.-M. Janik and V. Fresnaud, “A spectral approach to estimate the INL of A/D converter,” *Computer Standards & Interfaces*, vol. 29, no. 1, pp. 31–37, 2007.
- [7] A. C. Serra, M. F. da Silva, P. M. Ramos, R. C. Martins, L. Michaeli, and J. Šaliga, “Combined spectral and histogram analysis for fast ADC testing,” *IEEE Transactions on Instrumentation and Measurement*, vol. 54, no. 4, pp. 1617–1623, 2005.
- [8] V. Kerzérho, P. Cauvet, S. Bernard, F. Azaïs, M. Comte, and M. Renovell, “A novel DFT technique for testing complete sets of ADCs and DACs in complex SiPs,” *IEEE Design and Test of Computers*, vol. 23, no. 3, pp. 234–243, 2006.
- [9] V. Kerzérho, S. Bernard, P. Cauvet, and J. M. Janik, “A first step for an INL spectral-based BIST: the memory optimization,” *Journal of Electronic Testing: Theory & Applications*, vol. 22, no. 4–6, pp. 351–357, 2006.
- [10] D. Belega, M. Ciugudean, and D. Stoiciu, “Choice of the cosine-class windows for ADC dynamic testing by spectral analysis,” *Measurement*, vol. 40, no. 4, pp. 361–371, 2007.
- [11] L. Zhu, H. Ding, and K. Ding, “Phase regression approach for estimating the parameters of a noisy multifrequency signal,” *IEE Proceedings: Vision, Image and Signal Processing*, vol. 151, no. 5, pp. 411–420, 2004.





**Hindawi**

Submit your manuscripts at  
<http://www.hindawi.com>

